CHAPTER 6

Dust grain composition and properties around Young Stars

The presence of crystalline silicates has been detected in the circumstellar environment of several young stars in the recent past and there is evidence of silicon carbide (SiC) detection in the envelope of pre-main sequence star SVS13. In this chapter, we probe the presence of SiC in the dust around protoplanetary disks in a sample of young stars. We have modelled the linear polarization of composite dust grains in the mid-infrared (MIR: 8–13 μm) using silicates as host with various inclusions of SiC and graphites using the Discrete Dipole Approximation (DDA) and the Effective Medium Approximation (EMA) T-Matrix methods. The dust grain models have been compared with polarimetric observations made using CanariCam at the Gran Telescopio Canarias (GTC). We interpret the composition and properties of dust grains in our sample of stars based on the shape, size, composition, and fraction of inclusions by volume in our dust grain models.

6.1 Introduction and Motivation

Herbig Ae/Be stars, first identified by Herbig (1960) [187], are young (1–10 Myr) objects in the pre-main sequence having masses between 2–10 $M_{\odot}$. They are usually enclosed by a disk and/or a gaseous, dusty envelope since they form a part of the process of star formation [188]. Due to the infrared excess arising from the disk/envelope of Herbig stars [188, 189], they are often regarded as the massive analogues to young lower mass T-Tauri stars [190]. Meeus et al. (2001) [191] suggested that circumstellar disks surrounding Herbig stars could be categorized into two main groups: Group I comprising of sources showing strong infrared excesses having flared disks (mostly Herbig Ae stars) and Group II comprising of sources that show modest infrared excesses having flatter, self-shadowed disks (mostly Herbig Be stars) [192, 193]. The disk properties in Group I Herbig Ae stars have been observed to be very similar to T-Tauri stars [194, 195].

The study of protoplanetary dust in these young stars gives us an opportunity to understand massive star formation as well as planet formation processes [195] and the observation of large infrared excess makes mid-infrared (MIR) polarimetry an ideal tool to study their dust grain properties. Polarization is represented as the difference between the parallel and perpendicular components of extinction efficiency which are independently related to the dust optical constants [196]. The polarization profile (peak wavelength, shape, and strength) is highly susceptible to the specific shape, composition, as well as dust grain size and hence, the study of polarization across an absorption/emission feature can be very efficiently used to constrain these properties [197–199]. The polarization produced by dust grains in the interstellar medium (ISM) has been discussed in Section 1.1.3.

The composition of dust particles found in the protoplanetary disks around young stars can be reasonably assumed to be analogous to those in the ISM including silicates which are the most abundant species found in the ISM [33, 200]. The peak in absorption which arises due to Si–O bond stretching near MIR 10 μm has been widely studied and this feature, visible clearly in the linear polarization profile of interstellar dust grains, is attributed to non-spherical and aligned silicate dust grains [33, 196].

While amorphous silicates present in the ISM are mostly responsible for the 10 μm peak [201], Aitken et al. (1988) [202] observed an additional feature around 11 μm in the polarization profile towards a Class I Young Stellar Object (YSO), AFGL 2591, which was considered to have formed due to crystalline silicates similar to olivine. Separate studies have placed an upper limit on the abundance of silicates found in crystalline form in the ISM: 2.2% by Kemper et al. (2005) [31, 32] and 1% by Min et al. (2007) [33]. More recently, Wright et al. (2016) [199] have detected a 2.5–5% crystalline abundance towards the Galactic center based on three features at 11.1, 11.9 and 23.5 μm, which is consistent with the upper limit of Kemper et al. (2005) [32] and within the 3–5% limit set by Li et al. (2007) [203]. In case of protoplanetary disks, a review by Henning (2010) [204] has stated that amorphous silicates with various compositions are expected to be found in the outer regions while crystalline dust is expected towards the innermost (high temperature $\sim$ 1300 K) regions of the disk with the existence of annealed amorphous grains in-between the two regions. But the fact that crystalline material has also been observed in low temperature ($\sim$100 K) outer regions of disks means that there must either be some mechanism for large-scale transport/mixing or for low-temperature crystallization [190, 205].

The existence of crystalline silicates has now been observed in protoplanetary environments of both T-Tauri and Herbig Ae/Be stars [190, 206–211]. The interest in study of silicon carbide (SiC) as a potential dust constituent in protoplanetary disks arises from the fact that SiC, which is known to be formed in the circumstellar environment of AGB stars rich in carbon, has been found in pre-solar samples, i.e. all SiC grains are not destroyed in the ISM [212]. Hence, pre-solar SiC serves as an ideal tool to study new planetary systems and how they were formed with the same dust as that produced in ageing stars [213]. SiC has also been found as a dust constituent in comets and meteorites with evidence of pre-solar SiC grains to have been formed around the same time as graphites in the sample or even earlier [214–216]. On the basis of a feature occurring around 11 μm, Min et al. (2007) [33] found $\sim$3% SiC in interstellar dust grains with 9–12% of the silicon present in the SiC, but their inference was purely model-dependent. Several candidates have been identified for the 11 μm feature including SiC, hydrocarbons, water ice, carbonates, and crystalline silicates. Pott et al. (2008) [217] assigned the 11.3 μm feature to SiC, based on a slight bow in a low resolution (R$\sim$30) spectrum of SgrA IRS3. But the R$\sim$100 spectrum of the same target in Wright et al. (2016) [199] shows a distinct feature, which is much more consistent with crystalline silicates. The only detection of SiC based on the study of MIR polarization in the disk/envelope of a young star till date has been done by Fujiyoshi et al. (2015) [198] for SVS13. Hence, this detection has motivated us to investigate for evidences of silicon carbide (SiC) in the circumstellar environment of young stars.

In this work, the presence of SiC in protoplanetary disks around young stars has been probed by studying the effects of grain shape, size, composition, and volume fraction of inclusions on the polarization profile in the MIR within the 8-13 μm wavelength range.

6.2 Sample of Observations

Li et al. (2018) [218] have studied the magnetic fields of protoplanetary disks by measuring the MIR polarization of pre-main sequence stars using CanariCam which is a high-resolution MIR imaging instrument (7.5-25 μm) mounted over the 10.4 metre reflecting telescope, Gran Telescopio Canarias (GTC), situated at La Palma, Spain [82, 83]. It has spectroscopic, coronagraphic and polarimetric capabilities and has been constructed such that it reaches the telescope's diffraction limit at MIR wavelengths. The instrument details of CanariCam have been discussed in Section 1.2.2 while the details of observation and data reduction have been presented in Zhang et al. (2017a,b) [219, 220] and Li et al. (2018) [218].

The observations made by Li et al. (2018) [218] at 8.7 μm, 10.3 μm and 12.5 μm were selected such that they could sample the 10 μm silicate polarization feature which is ideally what we are trying to study in this work. They have separated the emission and absorption components of the star sample depending on the difference in polarization spectra across the 10 μm peak. We have used the polarimetric data of two Herbig Be stars and one T-Tauri star showing polarization in absorption from the sample of observations made by them.

Some details of the three stars as compiled by Li et al. (2018) [218] are shown in Table 6.1. The distances are given in parsec (pc), mass in terms of solar mass ($M_\odot$) and the age is given in million years (Myr). The absorption feature around 10 μm has been denoted as 'Abs' in the last column of Table 6.1. The details of polarization position angle (θ) measured by Li et al. (2018) [218] for the three stars at 8.7, 10.3 and 12.5 μm are shown in Table 6.2.

Table 6.1: Details of the two Herbig Be stars and one T-Tauri star in the sample observed by Li et al. (2018) [218].

Object	Distance (pc)	Mass ($M_\odot$)	Age (Myr)	10 μm Silicate Feature Type
MWC 1080A	1000	20.6	0.22	Abs
MWC 297	250	10	1	Abs
HL Tau	140	0.7	1	Abs

Table 6.2: The polarization position angles (θ) measured by Li et al. (2018) [218].

Wavelength	8.7 μm	10.3 μm	12.5 μm
Object		Observed θ (degree)	
MWC 1080A	110±1	104±1	71±10
MWC 297	80±19	74±7	91±26
HL Tau	88±2	89±1	94±3

MWC 1080A and MWC 297 are massive Herbig Be stars while HL Tau is a T-Tauri star which is the closest in our sample at 140 pc right before MWC 297 which is at a distance of 250 pc ([218] and references therein). MWC 1080A is comparatively a very young star [221] but all three show significant polarization in absorption. The two Herbig Be stars are surrounded by massive envelopes and seem to be still associated with the remains of their original molecular clouds [195, 218, 221]. Even HL Tau is know to be enclosed by a torus-shaped dusty envelope [222] and the polarization observed in absorption for these three stars has been attributed to their torus/envelopes surrounding the protoplanetary disks with all of them showing peak absorption in intensity and maximum polarization around 10.3 μm.

While the polarization profiles for MWC 297 and HL Tau show a sharp rise at 10.3 μm with subsequent fall to at least half this value on either side of the peak at 8.7 μm and 12.5 μm, the polarization value is significantly high towards 12.5 μm in case of MWC 1080A (as seen in Table 4, Li et al. (2018) [218]), i.e. there is a shift in peak value towards 11 μm which is usually seen in the presence of larger grains or crystalline particles [191].

6.3 Composite dust grain models

As discussed in Section 1.1.4, composite dust grain models which expect dust grains to be comprised of aggregates of carbonaceous particles and silicates are quite prevalent in literature [39, 67, 68]. Gupta et al. (2016) [91] have recently modelled spheroidal composite dust grains made of silicate as the host material with silicon carbide (SiC) and graphite as inclusions. They have studied the effects of change in axial ratio, size, porosity, and inclusions to the absorption efficiencies of dust grains in the 5-25 μm range with particular interest towards the 10 μm silicate feature observed in the MIR.

We have used a similar approach here as Gupta et al. (2016) [91] and varied the following parameters to obtain the absorption efficiencies and subsequently the linear polarization of the spheroidal dust grains.

Dust grain composition

For our composite model calculations, the host spheroid has been set to be made up of silicates with inclusions of either silicon carbide (SiC) or graphite (Gr) at a time. The sites external to the grain are assumed as vacuum and internal sites are given to the silicate host. Although C-rich AGB stars are the primary source for SiC production [223], it has also been detected in interplanetary dust particles (IDPs) and meteorites [224, 225]. More recently, Fujiyoshi et al. (2015) [198] have identified SiC to be a major component of the protoplanetary disk/envelope of dust around binary star system SVS13. They have modelled the polarization in SVS13 using amorphous silicates with SiC inclusions which motivated us to include SiC for our calculations as well. Graphite has been used since it is one of the prime candidates for the 2175 Å ultraviolet bump [97] observed in the extinction curve of the Galaxy. Alonso-Albi et al. (2009) [195] have successfully used a silicate/graphite mixture to model the dust in protoplanetary disks in a sample of Herbig Be stars. A significant amount of amorphous carbon or graphitic material is also found in the diffuse ISM (∼30% by mass) in addition to the abundance of amorphous silicates. Since studies [226, 227] have found dust grains to be fluffy and porous in nature, we have taken porous silicate based dust grains into consideration as well for our models. In addition, IDPs have also been found to consist of porous aggregates [228–230].

Axial ratio (AR)

We have used oblate (axial ratio>1) spheroids since interstellar extinction curves produced using models with grains in the form of oblate spheroids have been seen to show best fits with observed data [231]. Good fits have been observed by Henning & Stognienko (1993) [232] across 10 μm and by Kim & Martin (1995) [55] in the near-IR using such models. In fact, dust grains are required to be non-spherical in order to produce linear polarization via dichroism [57, 58]. Recently, Fujiyoshi et al. (2015) [198] have used oblate spheroids with axial ratio 2 to successfully model the protoplanetary disk polarization in SVS13. Hence, we have used three values of the axial ratio (AR) for our spheroidal grains, AR = 1.33, 2.0 and 1.5 which correspond to N = 9640, 14440 and 25896 dipoles respectively as detailed in Gupta et al. (2016) [91].

Grain radius & size integration

Fujiyoshi et al. (2015) [198] had considered a grain radius of up to 0.5 μm for protoplanetary disks in the MIR based on the Rayleigh approximation (grain size$\ll$wavelength). Min et al. (2007) [33] mention that the actual size of a particle is not important to determine the spectral shape in absorption/emission as long as it is in the Rayleigh domain. Hence, the absorption efficiencies have been calculated within the Rayleigh approximation using a grain size, a_{min}=0.1 μm to a_{max}=0.5 μm, where 'a' represents the radius of a sphere such that it's volume is equal to that of the dust grain spheroid. The details of particle size distribution are provided in Gupta et al. (2016) [91].

Volume fraction of inclusions

Alonso-Albi et al. (2009) [195] have made use of a grain mixture comprising of 86% silicates and 14% graphites for protoplanetary disks around Herbig Be stars. In this work, we have used three different fractions by volume, f = 0.1 (10%), 0.2 (20%) and 0.3 (30%) for SiC, graphite as well as porous grain inclusions (in compliance with earlier findings [91, 195]).

A composite grain model with AR = 1.33, i.e. N = 9640 dipoles and having f = 0.1 (90% silicates with 10% inclusions) is illustrated in Figure 6.1. We have also varied the polarization position angle (θ) parameter for our models using three values: 45, 60 and 90 degrees. The amorphous/astronomical silicate and graphite refractive indices used in our dust models have been obtained from Draine (2003) [233] while the SiC optical constants have been taken from Pegourie et al. (1988) [234].

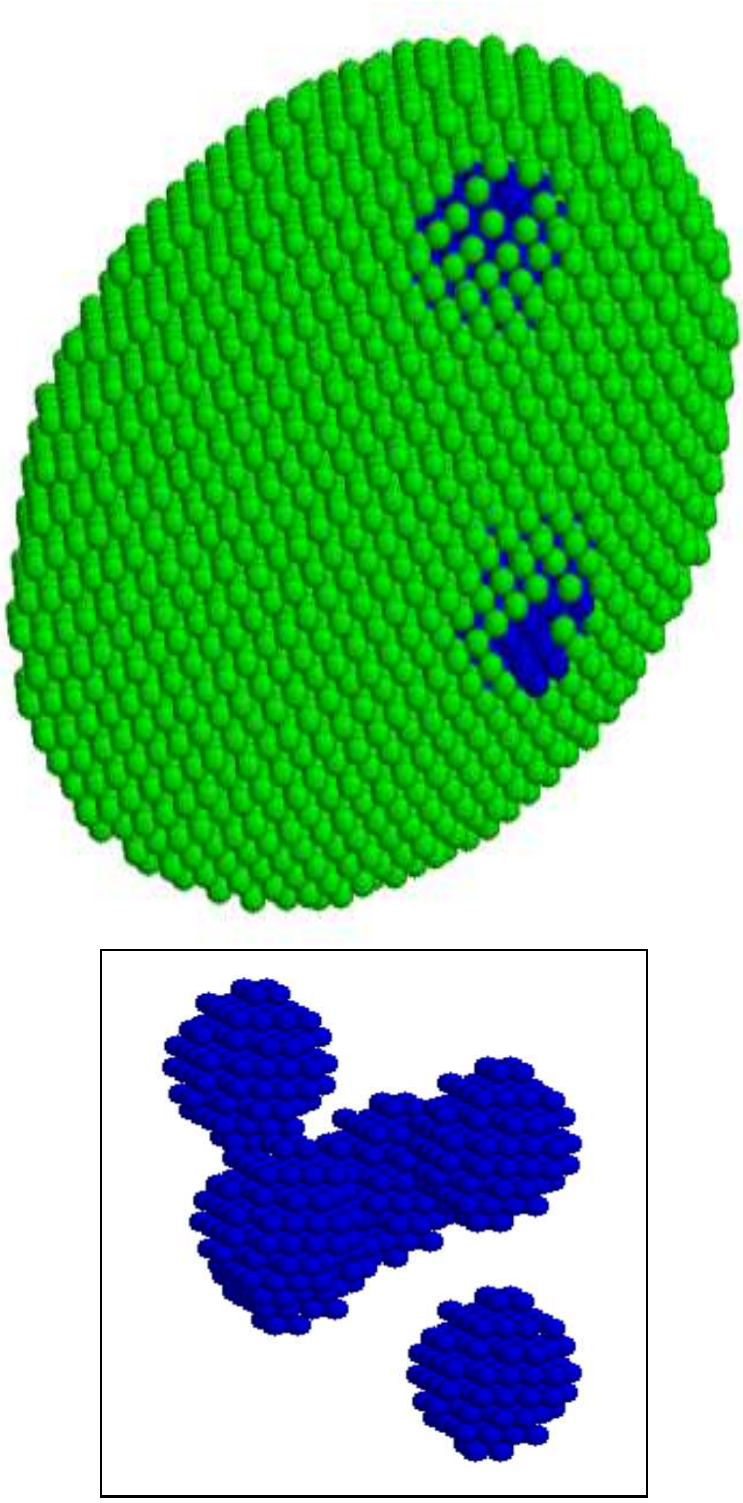

Figure 6.1: An oblate spheroidal composite dust grain model where the host material (silicate) is shown in green having an axial ratio (AR) = 1.33 with f = 0.1 (inclusions by volume). The inclusions are shown as blue implants in the upper panel and separately in magnified form in the lower panel. We are able to see only those inclusions in the upper panel which are located towards the perimeter of the spheroid while the rest are obstructed from our view.

6.4 Data analysis and Results

As discussed in Section 1.3.3, in the absence of a precise theory for the study of composite dust grain properties, we take the help of various approximation techniques such as the Effective Medium Approximation (EMA) and the Discrete Dipole Approximation (DDA) to model the scattering by non-spherical dust grains. The EMA method [92] uses T-Matrix which is based on Mie theory to determine the optical properties of small composite particles. It has a limitation in case of inhomogeneous particles because it uses a homogeneous particle with a single averaged optical property (refractive index, dielectric constant) to replace the original inhomogeneous one [93–95]. The DDA [96] method works very well for inhomogeneous particles taking into consideration the effects of various irregularities (shape, surface roughness, internal structure of grains). It represents an arbitrarily shaped composite dust grain in an array form with dipole elements which will experience a polarization whenever an electromagnetic radiation is incident and also due to oscillation of the rest of the dipoles. The interaction and superposition of these two polarization components causes scattering cross sections and extinction [97]. In spite of it's limitations, EMA is very convenient for large size parameters and complex refractive indices where DDA poses a computational challenge.

We have calculated the dust grain absorption efficiencies and the polarization in the 8-13 μm range using both DDA and EMA based composite models. We have used DDSCAT version 6.1 developed by Draine & Flatau (2003) [235] and the T-Matrix code developed by Mishchenko et al. (2002) [236] which were modified subsequently by Gupta et al. (2005) [231] and Vaidya & Gupta (2009) [237] for our DDA and EMA model calculations respectively. In our composite dust grain models, it has been observed that the inclusion of SiC leads to a longward shift in peak while the inclusion of graphite leads to a shortward shift of peak wavelength from 10 μm, as disussed in Gupta et al. (2016) [91].

We have compared the polarization data for MWC 1080A, MWC 297 and HL Tau observed by Li et al. (2018) [218] with the calculated linear polarization from our models. The best fit values and details of various parameters considered in our models for each of the observed stars for DDA based calculations are presented in Table 6.3 and for EMA T-Matrix model calculations are presented in Table 6.4. We have shown the corresponding best fit plots for the three stars in Figures 6.2, 6.3 and 6.4.

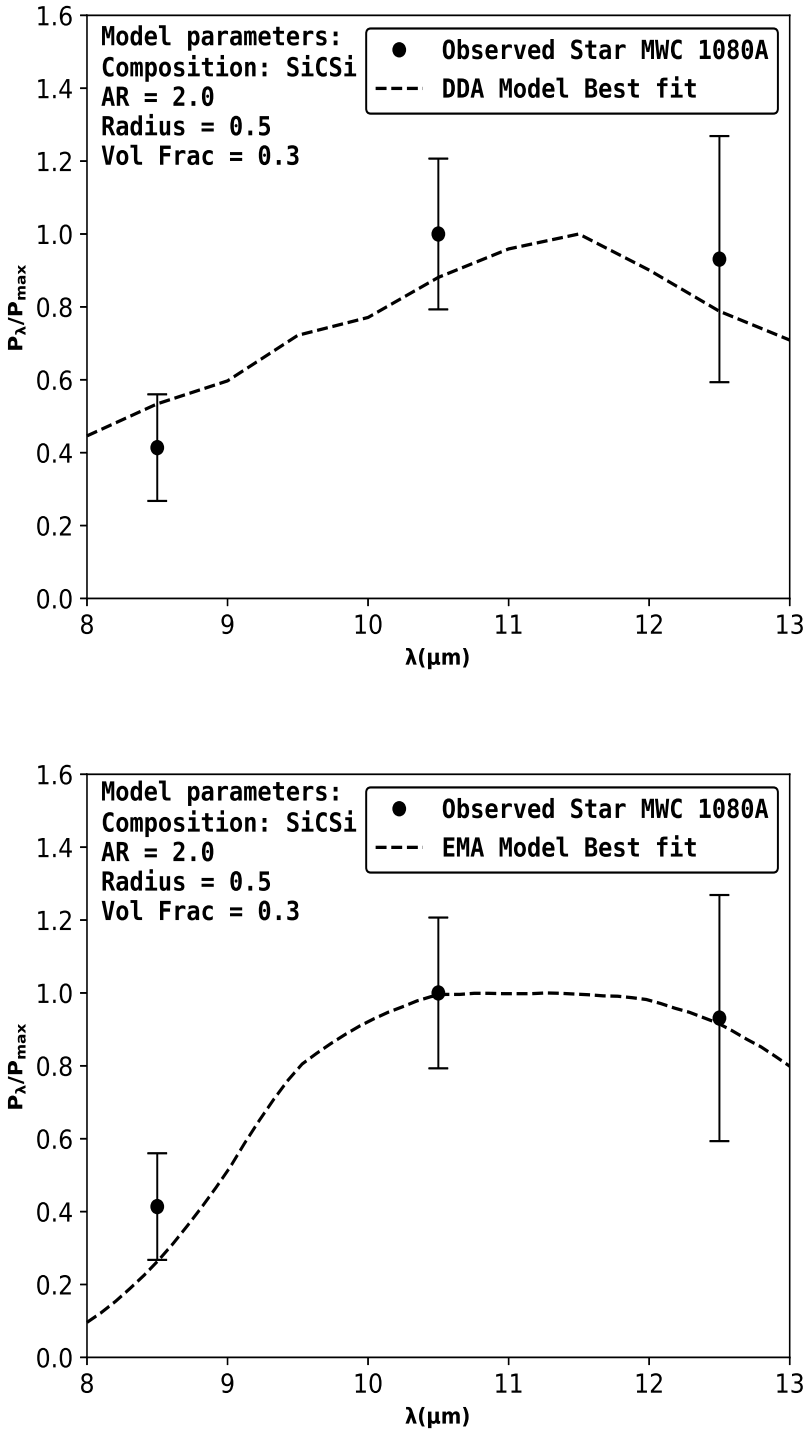

Figure 6.2: DDA (top panel) and EMA (bottom panel) based composite dust grain models with various combinations showing best fits to the observed star MWC 1080A.

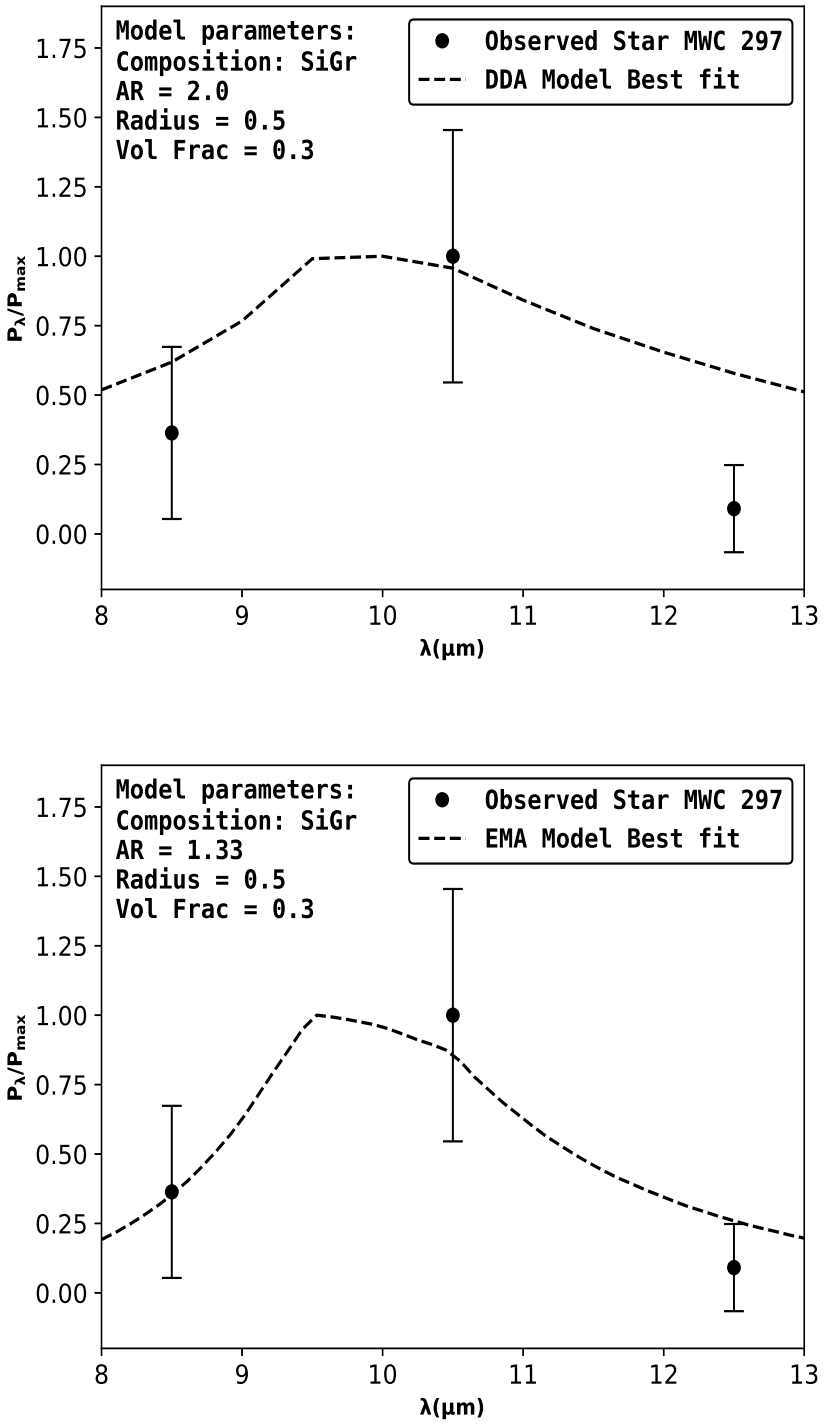

Figure 6.3: DDA (top panel) and EMA (bottom panel) based composite dust grain models with various combinations showing best fits to the observed star MWC 297.

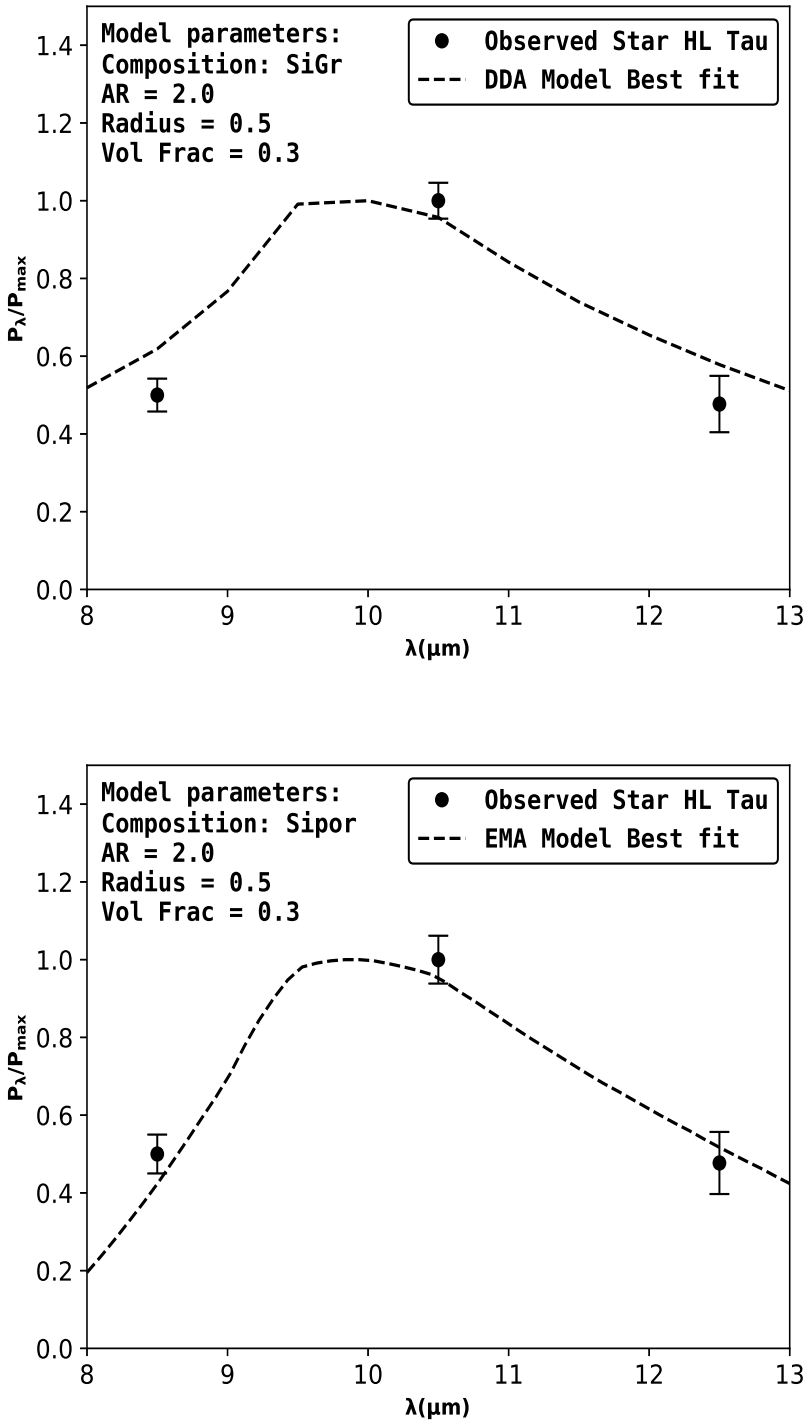

Figure 6.4: DDA (top panel) and EMA (bottom panel) based composite dust grain models with various combinations showing best fits to the observed star HL Tau.

Table 6.3: Details of best fit DDA based model parameters to the observed stars.

Object	Material Composition	AR	Size (μm)	Volume Fraction	θ (degree)
MWC 1080A	SiCSi	2.0	0.5	0.3	90
MWC 297	SiGr	2.0	0.5	0.3	90
HL Tau	SiGr	2.0	0.5	0.3	90

Table 6.4: Details of best fit EMA T-Matrix based model parameters to the observed stars.

Object	Material Composition	AR	Size (μm)	Volume Fraction	θ (degree)
MWC 1080A	SiCSi	2.0	0.5	0.3	90
MWC 297	SiGr	1.33	0.5	0.3	90
HL Tau	SiPor	2.0	0.5	0.3	90

6.5 Discussion and Conclusions

The results in Tables 6.3 and 6.4 show that composite models comprising of silicate as host with inclusions of SiC (f = 0.3) fit the observed MWC 1080A polarimetric data reasonably well for both DDA and EMA based models (Figure 6.2). On the other hand, the silicate/graphite mixture shows best fit to the observed MWC 297 polarization in both cases (Figure 6.3) while showing a good fit to HL Tau only in case of the DDA based model (Figure 6.4). The porous silicate model shows a better fit to the HL Tau polarization when computed using the EMA method. The other exception we find in case of MWC 297 best fits is the difference in the axial ratio for DDA and EMA based models (AR = 2.0 and 1.33 respectively). The DDA approach is, of course, more reliable since it is rigorous and incorporates particle inhomogeneities which EMA fails to do as discussed earlier. For all three objects, both the DDA and EMA-TMatrix models seem to best fit the observations at a polarization position angle, θ = 90 degree.

For all three young stars, we find elongated spheroidal shaped grains (AR = 2.0) with an effective radius of 0.5 μm to best fit the observations. As mentioned earlier, the grain size falls within the limits of Rayleigh approximation. Moreover, it has been observed that the dust grain size towards the inward regions of a protoplanetary disk is larger than those further out [194]. Alonso-Albi et al. (2009) [195] state that the distance from a star could very well determine the dust grain growth rate as well as the grain composition. They have given models with a maximum grain radius, a_{max}=1 cm for grains in the midplane of the disks in MWC 1080A and MWC 297 and a_{max}=100

μm and 1 μm for grains in the disk surface of each star respectively. However, it is known that HL Tau [238], as well as both these Herbig Be stars are associated with massive envelopes [195, 218, 221] which seem to be originators of the MIR absorptive polarization. If dust grain growth is indeed dependent on the distance from a star, the nature and size of dust grains found in such envelopes will resemble smaller ISM dust grains more closely than larger sized grains formed as a result of dust coagulation in the disks. In fact, it has been assumed that the dust grain growth from submicron to micron size takes place slowly over the course of a few million years [197]. Since MWC 297 and HL Tau are around 1 Myr in age (Table 6.1), it can be safely assumed that the typical dust grains in their envelope are still sub-micron sized. This assumption fits even better to the case of MWC 1080A which is still at a very young age of 0.22 Myr (Table 6.1).

In addition to the larger grain size, the flatness/shift of the typical 10 μm feature can also be caused due to the existence of crystalline silicate grains [197, 239]. In such cases, although the grain size is small, a flat feature may be caused due to summing up of all the crystalline peaks, hence giving an impression of a feature caused by an amorphous larger sized grain. We have observed a silicate/graphite mixture in the dusty envelope around MWC 297 (Figure 6.3) which agrees with the observations of a similar mixture in the MWC 297 disk made by Alonso-Albi et al. (2009) [195]. However, Li et al. (2018) [218] favour a model for the MWC 297 spectrum which incorporates combined polarised emission and absorption of silicate grains and it indeed fits the polarization data better than our model where we assume polarization only in absorption. We have observed a similar silicate/graphite mixture around HL Tau from our DDA based calculations (Figure 6.4). In contrast, the EMA based calculations show a porous silicate model to better fit with HL Tau observations which is in line with the pure silicate absorption model put forward by Li et al. (2018) [218] for the same target. For both MWC 297 and HL Tau, the best fit value of polarization angle (θ = 90 degree) is quite close to the position angles measured by Li et al. (2018) [218] as seen from Tables 6.2, 6.3 and 6.4; taking into account the uncertainties in observations at 8.7, 10.3 and 12.5 μm.

The SiC and silicate mixture which we have observed for MWC 1080A does not agree with the surface/midplane dust models given by Alonso-Albi et al. (2009) [195] for a silicate/graphite mixture. The deviation in results could be attributed to their simple model with different grain size distribution and also to the MWC 1080A polarization observed by Li et al. (2018) [218] which seems to arise from the envelope rather than the disk surface/midplane.

Li et al. (2018) [218] favour a pure absorption model with silicates only for MWC 1080A but it does not fit the 12.5 μm data which our SiC model does. The best fit polarization angle (θ = 90 degree) for our model lies midway between the position angles measured at 8.7 μm (110±1 degree) and 12.5 μm (71±10 degree) for MWC 1080A (Table 6.2). However, as noted by Li et al. (2018) [218], MWC 1080 seems to be a special case and the polarization angle observed deviates from models, in particular, the value at 12.5 μm, since it has a larger observational error. Such an occurrence of polarization due to absorption beyond the typical 10 μm feature was observed by Aitken et al. (1988) [202] which was considered to be due to the presence of crystalline silicates peaking at 11.2 μm. Min et al. (2007) [33] state that SiC grains that are irregular in shape show a broad feature in the spectra which peaks near 11.25 μm. Since we have indeed observed spheroidal silicate grains with AR = 2.0 having SiC inclusions to show such a broad feature peaking near 11.3 μm with significant polarization observed at 12.5 μm (Figure 6.2), we can assume the observed polarization in MWC 1080A to have been caused due to the SiC component present in the dust grains. Since MWC 1080A is a very young star with a small disk size, most of the observed polarization is caused due to the envelope which consists of material flowing in from the ISM. Moreover, multiple evidence has been found of the occurrence of crystalline silicates in cold outer shells/disks of Herbig stars [240] with separate mechanisms proposed for either transport/mixture of such dust to the outlying regions or for the formation of silicates in crystalline form in low temperature disks/envelopes due to shocks [190, 240].

The possible detection of SiC in the envelope of MWC 1080A here is very interesting due to the fact that there has only been one evidence of SiC detection while studying the MIR polarization in absorption which was made by Fujiyoshi et al. (2015) [198] for SVS13. We have checked the validity of our composite dust models for the same observations as shown in Figure 6.5.

Our DDA based calculations give a model with SiC, having 0.3 volume fraction of inclusions, for oblate spheroidal dust grains (AR = 1.5) of effective radius 0.5 μm to best fit the SVS13 polarization data. The EMA based calculations are in agreement to the type of inclusion, i.e. SiC, but vary in the degree of oblateness (AR = 2.0) and volume fraction of inclusions (0.2). Fujiyoshi et al. (2015) [198] had found similar results with an EMA based model having SiC inclusions, which is in agreement with our models. They had found an AR = 2.0 and volume fraction of inclusions 0.25 as best fit parameters when using the refractive indices of α-SiC given by Pegourie et al.

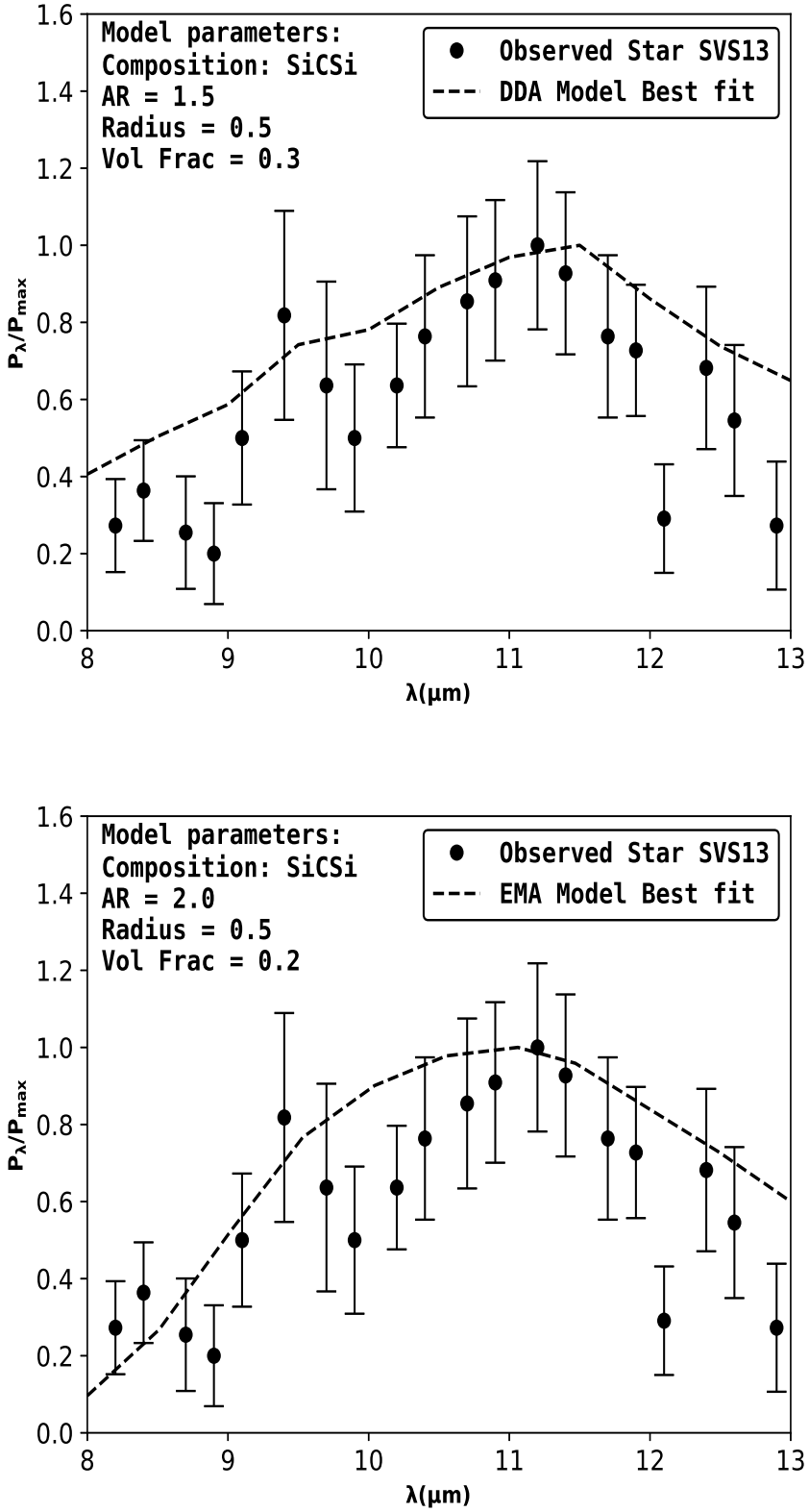

Figure 6.5: Composite grain models: DDA (top panel) and EMA (bottom panel) models with various combinations showing best fits to observed star SVS13 [198].

(1988) [234], which is the same one we have used here. The notable difference is only in the AR between our DDA based model and the EMA based results obtained by Fujiyoshi et al. (2015) [198] as supported by our calculations.

While most cases of crystalline silicate detection have been reported in emission [190, 210, 211], recent studies have shown a considerable number of such features in absorption as well [198, 199, 241]. All three objects in our sample of study: MWC 1080A, MWC 297 and HL Tau, show polarization in absorption but only the MWC 1080A polarization seems to have been caused due to SiC mixed with silicates. The dust grains accountable for the crystalline silicate features in absorption seem to originate in outer regions which are cold [198, 199]. This agrees very well with the MIR polarization in absorption originating from the outer envelope around MWC 1080A.

Therefore, we conclude that there is a possibility of silicon carbide (SiC) grains being present in the outer disk or envelope around MWC 1080A. Our results are limited by the lack of observed polarimetric data between 10.3 and 12.5 μm, the availability of which would add more credibility to the results obtained in this work. There is also a prospect of exploring the possible contribution of polycyclic aromatic hydrocarbon (PAH) molecules, which has already been detected for MWC 1080A [220], with the availability of reliable MIR polarization data for these objects.